Determining the probability of hemiplasy in the presence of incomplete lineage sorting and introgression

Mark S. Hibbins*, Matthew J.S. Gibson*, and Matthew W. Hahn*,†

*Department of Biology and †Department of Computer Science, Indiana University, Bloomington, IN 47405

ABSTRACT

The incongruence of character states with phylogenetic relationships is often interpreted as evidence of convergent evolution. However, trait evolution along discordant gene trees can also generate these incongruences – a phenomenon known as hemiplasy. Classic phylogenetic comparative methods do not account for discordance, resulting in incorrect inferences about the number of times a trait has evolved, and therefore about convergence. Biological sources of discordance include incomplete lineage sorting (ILS) and introgression, but only ILS has received theoretical consideration in the context of hemiplasy. Here, we derive expectations for the probabilities of hemiplasy and homoplasy with ILS and introgression acting simultaneously. We find that introgression makes hemiplasy more likely, suggesting that methods that account for discordance due to ILS alone will be conservative. We also present a method for making statistical inferences about the relative probabilities of hemiplasy and homoplasy in empirical datasets. Our method is implemented in the software package *HeIST* (Hemiplasy Inference Simulation Tool), and estimates the most probable number of transitions among character states given a set of relationships with discordance. *HeIST* can accommodate ILS and introgression simultaneously, and can be applied to large phylogenies. We apply this tool to a phylogeny of New Guinea lizards that have evolved green blood from a red-blooded ancestor, and find that hemiplasy is likely to explain the observed trait incongruence.

INTRODUCTION

Convergent evolution of the same phenotype in distantly related species provides some of the most compelling evidence for natural selection. Comparative inferences of convergence require that the species history is known (Felsenstein 1985). Such methods implicitly assume that the loci underlying convergent traits also follow the species history. However, gene trees at individual loci can disagree with each other and with the species phylogeny, a phenomenon known as gene tree discordance. While genomic data allow us to overcome many technical sources of discordance (Delsuc et al. 2005, Dunn et al. 2008, Misof et al. 2014), discordance also has biological causes (Degnan & Rosenberg 2009), and remains a common feature of phylogenomic datasets (Pollard et al. 2006, Fontaine et al. 2015, Pease et al. 2016, Novikova et al. 2016, Wu et al. 2018).

Gene tree discordance has two main biological causes: incomplete lineage sorting (ILS) and introgression. ILS is the failure of lineages to coalesce within a population before reaching the next most recent ancestral population, looking backwards in time. The probability of discordance due to ILS is a classic result of the multispecies coalescent, and depends on the population size and the length of time in which coalescence can occur (Hudson 1983, Pamilo & Nei 1988). More recently, the classic multispecies coalescent model has been extended to include introgression (a term we use to encompass hybridization and subsequent gene flow), in a framework called the "multispecies network coalescent" (Yu et al. 2012, Yu et al. 2014, Wen et al. 2016). In this model, species relationships are modelled as a network, with introgression represented by horizontal reticulation edges. Individual loci probabilistically follow or do not follow the reticulation edge, after which they sort according to the multispecies coalescent process. A major advantage of this approach is that ILS and introgression can be modelled simultaneously (reviewed in Degnan 2018), allowing for more detailed study of the consequences of discordance.

Importantly, discordant gene trees can lead to the appearance of apparently convergent traits. This is because discordant gene trees have internal branches that do not exist in the species tree. If a mutation occurs along such a branch at a locus controlling trait variation, it may produce a pattern of character states that is incongruent with the species tree. Incongruent trait patterns are the basis for inferences of convergent evolution ("homoplasy"), and thus this phenomenon has become known as hemiplasy (Avise & Robinson 2008). Since hemiplasy can produce the same kinds of trait incongruence as homoplasy, failing to account for gene tree discordance can generate misleading inferences about convergence (Mendes & Hahn 2016, Mendes et al. 2016). Studies in systems with widespread discordance have found that hemiplasy is a likely explanation for many patterns of incongruence (Copetti et al. 2017, Wu et al. 2018, Guerrero & Hahn 2018).

The problem of hemiplasy makes it clear that robust inferences about the evolution of traits must account for gene tree discordance (Hahn & Nakhleh 2016). Recent work has provided expressions for the probabilities of hemiplasy and homoplasy (Guerrero & Hahn 2018), allowing

for an assessment of whether a single transition (hemiplasy) or two transitions (homoplasy) is more likely to explain trait incongruence. This model shows that the most important factors contributing to a high risk of hemiplasy relative to homoplasy are a short internal branch on the species tree (which increases the rate of gene tree discordance), and a low mutation rate (which reduces the probability of the multiple independent transitions needed for homoplasy). However, applying this model in present form to empirical phylogenetic data faces two major limitations. First, incomplete lineage sorting is the only source of gene tree discordance considered, excluding scenarios with gene flow. Second, the model is limited to evolution along a three-taxon tree, restricting calculations for the exact probability of hemiplasy in larger clades.

With genomic data now available for many species, it has become clear that introgression is a common phenomenon (Mallet et al. 2016). Introgression leads to different patterns of gene tree discordance than expected under ILS alone – specifically, minority gene tree topologies supporting a history of introgression are expected to become more common than those produced via ILS alone. These differences form the conceptual basis for common tests of introgression using genomic data (Reich et al. 2009, Green et al. 2010, Durand et al. 2011, Patterson et al. 2012, Pease & Hahn 2015). Introgression also affects the expected coalescence times between pairs of species (Joly et al. 2009, Brandvain et al. 2014, Hibbins & Hahn 2019, Hahn & Hibbins 2019). Pairs of species that have exchanged genes should have lower levels of sequence divergence, and therefore longer shared internal branches, than expected under ILS alone. These differences in the frequency and branch lengths of genealogies produced by introgression should meaningfully affect the probability of hemiplasy. Therefore, it is important that both sources of gene tree discordance be accounted for in models of trait evolution.

For trees with more than three taxa, the number of possible gene trees and mutational configurations that could explain a particular pattern of trait incongruence increases dramatically. To illustrate this problem, consider the case of green-blooded lizards from New Guinea (Figure 1; Rodriguez et al. 2018). A clade of 15 taxa contains both the green-blooded species and red-blooded species (the ancestral state). Given the phylogenetic distribution of the six green-blooded species—and no consideration of gene tree discordance—four independent transitions are necessary to explain this incongruence (Figure 1). However, the internal branches on this tree are short and discordance is likely. Individual loci could therefore group the green-blooded taxa into as few as one and as many as six separate clades. Depending on the history at loci affecting blood color, the distribution of green-blooded taxa could therefore be explained by anywhere from one to six mutations, and even more if we consider back-mutations. The one-mutation case represents a single transition due to hemiplasy along a branch that does not exist in the species tree, while the two- and three-mutation cases represent a combination of hemiplasy and homoplasy. Given the huge number of possible gene trees for 15 species (>213 trillion; Felsenstein 2004), and the large number of possible mutational events on these trees, an explicit mathematical approach to addressing these questions is not currently feasible.

Here we make two steps towards addressing these problems. First, we derive expressions for the probabilities of hemiplasy and homoplasy under the multispecies network coalescent for three taxa. Our results show that hemiplasy becomes increasingly likely relative to homoplasy as

introgression occurs at a higher rate and at a more recent time relative to speciation. We also show how this pattern is influenced by the direction of introgression. These results highlight the need to account for both sources of discordance in order to understand the origins of a trait incongruence. Second, we present a tool called *HeIST* (Hemiplasy Inference Simulation Tool) which uses coalescent simulation to dissect patterns of hemiplasy and homoplasy in larger phylogenies. This tool provides an estimate of the most likely number of transitions giving rise to an observed incongruence of binary traits, and accounts for both ILS and introgression. *HeIST* also contains a module for converting a phylogeny in units of substitutions per site into coalescent units using concordance factors, something that current methods for coalescent-based species tree inference cannot do for tip branches. Lastly, we apply *HeIST* to the phylogeny of green-blooded lizards, and find that hemiplasy is likely to explain the observed trait incongruence.

MATERIALS AND METHODS

A model for the probability of hemiplasy under the multispecies network coalescent

To study the effects of introgression on the probability of hemiplasy, we combine concepts from two previously published models: the "parent tree" framework of Hibbins & Hahn (2019), and the model of binary-trait evolution presented in Guerrero & Hahn (2018). Consider a rooted three-taxon tree with the topology ((A,B), C). We define t_1 as the time of speciation between lineages A and B in units of $2N$ generations, and t_2 as the time of speciation between C and the ancestor of A and B. We also imagine an instantaneous introgression event between species B and C at time t_m, which can be in either direction (C → B or B → C). We define the total genomic rate of introgression as δ, with δ_2 denoting the rate of C → B introgression, and δ_3 the rate of B → C introgression. The history described here is represented by the phylogenetic network shown in Figure 2 (top).

To make it easier to track the history of different gene trees, we imagine that a phylogenetic network can be split into a set of "parent trees" which describe the history at individual loci (Meng & Kubatko 2009, Liu et al. 2014, Hibbins & Hahn 2019) (Figure 2, bottom). Within each of these parent trees, which describe either the species history or the history of introgression, gene trees sort under the multispecies coalescent process. Loci follow the species history, referred to as parent tree 1, with probability $1 - (\delta_2 + \delta_3)$. With C → B introgression, some loci will follow an alternative history within parent tree 2, with probability δ_2. In parent tree 2, species B and C are sister and share a "speciation" time of t_m. B → C introgression causes loci to follow parent tree 3 with probability δ_3; in this history lineages B and C are sister and split at time t_m, while the split time of A and the ancestor of B/C is reduced to t_1. This reduction in the second split time in parent tree 3 occurs because the presence of loci from lineage B in lineage C allows C to trace its ancestry through B going back in time. Since B is more closely related to A than C, this allows C to coalesce with A at an earlier time (Figure 2).

Each parent tree can produce four gene trees under the multispecies coalescent process: one tree from lineage sorting, and three equally probable trees from incomplete lineage sorting. Each of

these gene trees has five branches along which mutations can occur: three tip branches, an internal branch, and an ancestral branch. Guerrero & Hahn (2018) provide exact expectations for the probability of a mutation on each branch of each genealogy in an ILS-only model. Before extending this framework to incorporate introgression, the ILS-only model will be briefly described here, using a slightly updated notation that will make it easier to include the effects of introgression.

Consider a binary trait that is incongruent with the described species tree, where species B and C have the derived state and A has the ancestral state. We denote λ_1, λ_2, and λ_3 as the tip branches leading to species A, B, and C respectively; λ_4 denotes the internal branch, and λ_5 the branch subtending the root. The notation $\nu(\lambda_i, \tau)$ represents the probability of a mutation on branch λ_i in genealogy τ. The rates of $0 \rightarrow 1$ and $1 \rightarrow 0$ mutations are assumed to be equal, and the rate among lineages is assumed to be constant. Finally, to describe individual genealogies, we use the notation XY_i, where X and Y denote the sister taxa, and the subscript i denotes the parent-tree of origin. In cases where a tree topology can be produced by either lineage sorting or ILS, a non-subscripted 1 or 2 is used, respectively. Under the ILS-only model, hemiplasy can only occur through a substitution on branch λ_4 of genealogy BC_1 (Figure 3). This occurs with the following probability:

$$P_e[BC_1] = \left(\frac{1}{3}e^{-(t_2-t_1)}\right)\nu(\lambda_4, BC_1)\prod_{i\neq 4}(1-\ \nu(\lambda_i, BC_1)) \quad (1)$$

(Guerrero & Hahn, 2018). Equation 1 has three components: the probability of observing genealogy BC_1, the probability that a mutation happens on the internal branch of that genealogy, and the probability that no other mutations occur. See the Supplement for the full expressions for each mutation probability.

Now consider the phylogenetic network described earlier and shown in Figure 2. At an introgressed locus, the parent tree topology is ((B,C), A), but could be either parent tree 2 or 3. Within each of these parent trees there are two possible gene trees that share this topology: one produced by lineage sorting and one produced by ILS where B and C are still the first to coalesce (Figure 3). While these trees have the same topology, their expected frequencies and internal branch lengths differ. These quantities also differ depending on the direction of introgression at the locus; i.e. whether the history follows parent tree 2 or 3.

We first consider the C → B direction of introgression, and genealogy $BC1_2$, which is the result of lineage sorting within parent tree 2. This gives:

$$P_e[BC1_2] = \left(1\ -\ e^{-(t_2-t_m)}\right)\nu(\lambda_4, BC1_2)\prod_{i\neq 4}(1-\ \nu(\lambda_i, BC1_2)) \quad (2)$$

While equation 2 has the same three core components as equation 1, there are several important differences. First, the gene tree probability is the probability of lineage sorting within parent tree 2, which differs from the probability of ILS within parent tree 1. Second, the lower bound of coalescence is t_m rather than t_1, resulting in a higher probability of lineage sorting in parent tree 2 as compared to parent tree 1. Third, because B and C coalesce more quickly in this tree, they share a longer internal branch, which means the probability of mutation on that branch is higher (see Supplement).

ILS within parent tree 2 produces gene tree $BC2_2$, in which B and C are the first to coalesce in the common ancestor of all three species. The probability of hemiplasy in this case is:

$$P_e[BC2_2] = \left(\frac{1}{3}e^{-(t_2-t_m)}\right)\nu(\lambda_4, BC2_2)\prod_{i\neq 4}(1-\ \nu(\lambda_i, BC2_2)) \quad (3)$$

In equation 3, the gene tree probability represents ILS in parent tree 2. This probability is lower than its equivalent in parent tree 1, again because t_m is the lower bound for coalescence. Since the upper bound to coalescence is the same (t_2), the probability of a mutation on the internal branch of this gene tree is the same as for BC_1 (the ILS topology within parent tree 1). To get the overall probability of hemiplasy due to both ILS and introgression, we weight the probability from each gene tree (equations 1-3) by the admixture proportion, giving the following:

$$P_e = (1-\ \delta_2)P_e[BC_1] +\ \delta_2(P_e[BC1_2] +\ P_e[BC2_2]) \quad (4)$$

From equation 4, we can see that introgression will increase the probability of hemiplasy over ILS alone (equation 1) whenever the probability of hemiplasy from parent tree 2 is higher than from parent tree 1 (i.e. $P_e[BC1_2] +\ P_e[BC2_2] >\ P_e[BC_1]$). This is true whenever $t_2 > t_m$ (see section 2 of the Supplement), which is by definition always true in this model.

Finally, we consider the probability of hemiplasy when introgression is in the direction B → C (represented by admixture fraction δ_3). As mentioned previously, this direction of introgression results in an upper bound to coalescence of t_1 rather than t_2. This is the primary difference between the directions of introgression, affecting both the expected gene tree frequencies and mutation probabilities (compare to equations 2 and 3):

$$P_e[BC1_3] = \left(1\ -\ e^{-(t_1-t_m)}\right)\nu(\lambda_4, BC1_3)\prod_{i\neq 4}(1-\ \nu(\lambda_i, BC1_3)) \quad (5)$$

and

$$P_e[BC2_3] = \left(\frac{1}{3}e^{-(t_1-t_m)}\right)\nu(\lambda_4, BC2_3)\prod_{i\neq 4}(1-\ \nu(\lambda_i, BC2_3)) \quad (6)$$

For the general probability of hemiplasy, including both directions of introgression, we now have:

$$P_e = (1-(\delta_2+\ \delta_3))P_e[BC_1] +\ \delta_2(P_e[BC1_2] +\ P_e[BC2_2]) + \delta_3(P_e[BC1_3] +\ P_e[BC2_3]) \quad (7)$$

Finally, we consider the probability of homoplasy. As described in Guerrero & Hahn (2018), there are two possible paths to homoplasy for a three-taxon tree where taxa B and C carry the derived state. The first is parallel 0 → 1 mutations on branches λ_2 and λ_3, and the second is a 0 → 1 mutation on branch λ_5 followed by a 1 → 0 reversal on branch λ_1. Both of these paths to homoplasy can happen on any possible genealogy, giving the following:

$$P_o =\ \sum_\tau\ p(\tau)\left[\nu(\lambda_2,\tau)\nu(\lambda_3,\tau)\prod_{i\neq 2,3}\left(1-\ \nu(\lambda_i,\tau)\right) +\ \nu(\lambda_1,\tau)\nu(\lambda_5,\tau)\prod_{i\neq 1,5}\left(1-\ \nu(\lambda_i,\tau)\right)\right] \quad (8)$$

where τ denotes the set of all possible gene trees. (Note that the sum inside equation 8 is multiplied by $\frac{1}{p(\tau)}$ in the main text of Guerrero & Hahn (2018). This is a typo, but the results presented from their model use the correct expression, $p(\tau)$.) This formulation can also be applied to the extended model with introgression, with the understanding that τ now also includes the gene trees produced by parent trees 2 and 3.

To understand the analytical effect of introgression on the relative risks of hemiplasy and homoplasy, we plotted the ratio P_e/P_o over a realistic range of admixture proportions, timings, and directions. The values of t_1 and t_2 were held constant at 1 and 3.5 coalescent units, respectively, with a population-scaled mutation rate of $\theta = 0.002$. These settings ensured a constant contribution of incomplete lineage sorting to the risk of hemiplasy, leading to a baseline ratio of hemiplasy to homoplasy, P_e/P_o, of 0.818 with no introgression. We varied the admixture proportion from 0-10%, and the value of t_m from 0.99 (just after the most recent speciation) to 0.01, for three different direction conditions: C → B only, B → C only, and equal rates in both directions.

***HeIST*: Hemiplasy Inference Simulation Tool**

As described above, it is possible to infer the most likely number of transitions for an incongruent trait while accounting for discordance in a rooted tree with three taxa. However, similar calculations are computationally difficult for larger numbers of taxa. Here, we present a tool built on top of the coalescent simulator *ms* (Hudson 2002) and sequence simulator *Seq-Gen* (Rambaut & Grassly 1997) that provides an intuitive way to explore parameter space with larger trees. Our tool, dubbed *HeIST* (Hemiplasy Inference Simulation Tool), takes a phylogenetic tree (including an option to specify introgression events) with observed character states as input, and returns a simulated distribution of the number of transitions necessary to explain those character states. The input phylogeny must be in coalescent units, but we also include a tool for converting trees given in units of substitutions per site to coalescent units, as long as branches are also associated with concordance factors (see next section).

HeIST uses *ms* to simulate a large number of gene trees from the specified species tree or species network, and then simulates the evolution of a single nucleotide site along each of these gene trees using *Seq-Gen*. Loci where the simulated nucleotide states match the character states observed on the species tree are taken as replicate simulations of the evolution of the trait being studied. In these focal cases, *HeIST* counts the number of mutations that occurred along the gene tree in each simulation. It also returns information on the frequency of tip vs. internal branch mutations, transition vs. reversal mutations, the distribution of gene tree topologies, and whether gene trees originate from the species branching history or introgression history. Finally, it returns a summary of how much hemiplasy is likely to contribute to observed character states, using Fitch parsimony (Fitch 1971) to obtain a homoplasy-only baseline for comparison. *HeIST* is implemented in Python 3 and the package/source code are freely available from https://github.com/mhibbins/HeIST.

Inferring the tip branch lengths of a phylogeny in coalescent units

Inferences made under the multispecies coalescent require branch lengths specified in coalescent units. However, most standard methods for building phylogenies infer branches in units of substitutions per site. Units of absolute time inferred from substitution rates using molecular clock approaches can be converted into coalescent units, provided that the generation time and effective population size are known. However, these parameters are sometimes not available or accurate for a given system. As an alternative, estimates of rates of gene tree discordance can be used to estimate internal branch lengths in coalescent units, but these provide no information about the lengths of tip branches. For example, the species tree inference software ASTRAL (Zhang et al. 2018) does not infer tip branch lengths, while the software MP-EST (Liu et al. 2010) adds branches of length 9 for every tip. These tip lengths are necessary to make accurate inferences about hemiplasy and homoplasy from empirical data, since they affect the probability of mutation on tip branches.

To ameliorate this problem, we have applied a simple regression approach for inferring tip lengths in coalescent units (see Bastide et al. 2018 for an alternative method). Our approach makes use of concordance factors: estimates of the fraction of concordant loci with respect to a particular branch in a species tree. Concordance factors come in two flavors: gene concordance factors (gCFs) (Gadagkar et al. 2005, Ane et al. 2007), which estimate the concordance of gene tree topologies, and site concordance factors (sCFs) (Minh et al. 2018), which do the same for parsimony-informative sites. In general, concordance factors estimated from quartets provide an estimate of $1 - {}^{2}/_{3}\, e^{-T}$, where T is the length of the internal branch in coalescent units. With concordance factors labelled on the internal branches of a tree in substitutions per site, the aforementioned formula can be used to obtain estimates of those same branch lengths in units of *2N* generations. A regression of the internal branch length estimates in both units can then be used to obtain a formula for unit conversion between them. This formula can subsequently be used to predict the tip branch lengths of the tree in coalescent units. As a final step in this process, the tree in coalescent units is smoothed, as *ms* requires the input tree to be ultrametric. *HeIST* does this using the smoothing method implemented in *ete3* (Huerta-Cepas et al. 2016), which redistributes the tree branch lengths so that the distance from the root to each tip is the same.

Our regression approach is implemented in *HeIST* and can be run as part of the overall hemiplasy analysis, or separately using the module "*subs2coal*".

Application of *HeIST* to New Guinea lizards

As a case study, we applied *HeIST* to a dataset of New Guinea lizards (Rodriguez et al. 2018). As described in the Introduction, the genus *Prasinohaema* contains six species that have evolved green blood from a red-blooded ancestor (Figure 1). Previous analyses of the species tree built from thousands of loci inferred that four independent transitions are necessary to explain the phylogenetic distribution of green-blooded species (Rodriguez et al. 2018). This conclusion is the same using any standard phylogenetic comparative method, whether ancestral state reconstruction is carried out using maximum likelihood (Rodriguez et al. 2018) or Fitch parsimony (this study). However, the phylogeny for this clade contains many short branches

(Figure 1), suggesting that a scenario involving at least some hemiplasy (in this case, 1-3 mutations) may be preferred over homoplasy-only scenarios when discordance is accounted for.

To address this question, we obtained the original dataset from the authors, consisting of 3220 ultra-conserved elements (UCEs) totalling approximately 1.3 Mb for 43 species. We down-sampled these species to 15 taxa in the clade including the green-blooded species and an outgroup (Figure 1). We constructed a concatenated maximum likelihood species tree, in addition to gene trees for each UCE, using RAxML version 8.2.12 (Stamatakis 2014). To verify the species tree topology for the 15-taxon subclade, we also constructed a tree with ASTRAL-III version 5.6.3 (Zhang et al. 2018). Site and gene concordance factors were calculated for this tree using IQ-TREE version 2.0 (Minh et al. 2020). To obtain the phylogeny in coalescent units, we employed the regression approach described above for unit conversion as implemented in *HeIST*. We then used *HeIST* to simulate 10^{10} loci from the lizard subclade containing green-blooded species, with a population-scaled mutation rate (θ) of 0.001. We also calculated *D*-statistics (Green et al. 2010) for 12 trios involving green-blooded taxa, and found no strong evidence of introgression (block bootstrap significance tests, Supplementary Tables S2 and S3). Therefore, our simulations did not include any introgression events.

RESULTS

Introgression makes hemiplasy more likely than incomplete lineage sorting alone

Using our model for the probability of hemiplasy, we examined the ratio P_e / P_o over a range of different introgression scenarios. We find that the probability of hemiplasy relative to homoplasy increases as a function of the admixture proportion and how recently introgression occurs relative to speciation (Figure 4). As mentioned in the Introduction, there are several possible reasons for these observed trends. The strongest effect on P_e / P_o comes from the admixture proportion: a higher proportion means more loci evolving under parent trees 2 and 3, which means higher frequencies of the genealogies where hemiplasy is possible (i.e. $BC1_2$, $BC2_2$, $BC1_3$, $BC2_3$). The range of simulated admixture proportions from 0 to 10 percent was meant to capture a biologically plausible range of values, though rates of introgression can sometimes be much higher than this (e.g. Fontaine et al. 2015). Even in this modest range, the effect on the probability of hemiplasy can be substantial. We found that an admixture proportion of 5% results in hemiplasy being anywhere from 1.5 to 4 times more likely than homoplasy (depending on the timing and direction of introgression; Figure 4). Given the baseline value of P_e / P_o with no introgression for our chosen parameters (0.818), this represents at minimum a doubling of the probability of hemiplasy relative to homoplasy.

The effect of the timing of introgression is more complicated, as it manifests in multiple ways. First, more recent introgression increases the values of $t_2 - t_m$ and $t_1 - t_m$, which in turn increases the degree of lineage sorting in parent trees 2 and 3, respectively. This leads to a higher frequency of gene trees where hemiplasy is possible. Second, the expected length of the internal branches in these two genealogies increases as introgression becomes more recent, which leads to a higher probability of mutations occurring on these branches. Third, since the total height of each tree is being held constant, more recent introgression reduces the lengths of the tip branches

leading to species B and C. This reduces the probability of homoplasy due to parallel substitutions, again making hemiplasy relatively more likely. Finally, the strength of the effect of the timing of introgression increases with the admixture proportion, since it is a property of introgressed loci; in other words, the values of of $t_2 - t_m$ and $t_1 - t_m$ do not matter unless loci follow a history of introgression.

The direction of introgression affects the relationship between the admixture proportion, the timing of introgression, and hemiplasy risk (Figures 4B and 4C). While hemiplasy becomes more likely than homoplasy with increased admixture in either direction, P_e / P_o is lower in any given part of parameter space for B → C introgression (Figure 4C). This is because the bounds of coalescence for parent tree 3 are t_1 and t_m, which are always closer in time than t_2 and t_m (Figure 2). The smaller internal branch in parent tree 3 leads to a higher rate of ILS, in addition to a shorter internal gene tree branch (and lower mutation probability) on genealogies that undergo lineage sorting in these histories. Finally, the timing of introgression has a stronger effect on P_e / P_o in the B → C direction (Figure 4C). This is likely because parent tree 3 is truncated relative to parent tree 2 (see Figure 2), and so the difference $t_1 - t_m$ makes up a proportionally larger part of the tree height.

The distribution of green-blooded New Guinea lizards is likely to have arisen from fewer than four transitions

We investigated the most likely number of transitions to green blood from a red-blooded ancestor in New Guinea lizards of the genus *Prasinohaema* (Rodriguez et al. 2018). Phylogenies constructed using RAxML (Figure 1) and ASTRAL (Supplementary Figure 1) recover the phylogeny published by Rodriguez et al. (2018), including the placement of green-blooded species, and also confirm the existence of very short internal branches. In line with this observation, site concordance factors estimated from UCEs indicate very high rates of discordance in this clade, with some approaching a star tree (i.e. all topologies having frequencies of 33%) (Figure 1, Supplementary Table 1). This strongly suggests that the apparent convergent evolution of the green blood phenotype has been affected by hemiplasy.

We used *HeIST* with the 15-taxon subclade containing the 6 green-blooded species to determine the most likely number of trait transitions. Using our branch length unit conversion tool *subs2coal*, we obtained a best fit line of $y = 0.3038 + 157.03x$ with an adjusted R^2 of 0.554 (Figure 5). This formula was used to predict the tip branch lengths of the lizard phylogeny in coalescent units, for input to *HeIST* (Figure S2). With four independent transitions required without discordance, there are three possible scenarios that involve at least one hemiplastic transition (Figure 6). The first is a hemiplasy-only scenario, in which all green-blooded species are grouped into a single monophyletic clade in a gene tree, and a single transition in the ancestor of this clade explains the observed distribution (Figure 6A). Out of 131 total simulated datasets matching the empirical distribution of green-blooded species, 40 (30.5%) correspond to this hemiplasy-only case. In the second case, the green-blooded species may be grouped into one or two clades in a gene tree, and there are two independent transitions—at least one of which must involve a discordant ancestral branch (Figure 6B). Since there are still multiple independent transitions, this case represents a combination of hemiplasy and homoplasy. 86 out of 131 focal

cases (65.6%) correspond to this scenario. In the third case, the green-blooded species are grouped into as many as three clades, with three independent transitions, at least one of which must be hemiplastic (Figure 6C). We observed four such cases (3.1% of focal cases). Finally, we observed one case (0.8% of cases) where four (Figure 6D) transitions led to the distribution of green-blooded species. These results strongly support the conclusion that, due to hemiplasy, the green-blooded phenotype arose from one or two independent transitions, rather than four.

Strikingly, 125 of 131 (~95%) focal cases involved a gene tree topology where the six green-blooded species were grouped as monophyletic, despite there being only 40 cases that involved a single mutation. This result suggests that, for this system, hemiplastic substitutions in general that lead to the observed trait distribution are much more likely to occur at loci where the gene tree groups the green-blooded species as monophyletic. Following the logic of "PhyloGWAS" (Pease et al. 2016), we checked biallelic sites in the UCE alignment and topologies from the UCE gene trees for a monophyletic clade of green-blooded lizards in order to identify regions potentially associated with variation in blood color. However, owing to missing data and the fact that the UCE dataset represents a small proportion of the genome, we did not find any such regions.

DISCUSSION

Phenotypic convergence among species can provide important evidence for natural selection. The molecular variation underlying this convergence can arise through independent mutations at the molecular level (Storz 2016). However, it has recently become clear that such cases of "true" convergence need to be distinguished from cases of apparent convergence due to hemiplasy (Hahn and Nakhleh 2016). Some effort has been made recently in this regard, through the use of coalescent simulation, summary statistics, and updated comparative approaches (Pease et al. 2016, Copetti et al. 2017, Guerrero & Hahn 2018, Wu et al. 2018). However, these approaches often assume incomplete lineage sorting as the only source of discordance, and cannot explicitly resolve the number of transitions required to explain a trait distribution while accounting for discordance. Here, we take two important steps towards addressing these problems by: 1) studying the effect of introgression on the risk of hemiplasy under the multispecies network coalescent, and 2) providing a tool that can infer the most probable number of transitions given a phylogenetic distribution of traits. We find that introgression increases the risk of hemiplasy over ILS alone, and uncover a likely hemiplastic origin for the evolution of green blood from a red-blooded ancestor in New Guinea lizards. While our work has important implications for studies of trait evolution, it also carries numerous limitations and simplifying assumptions, which suggest logical next steps for further work. Below we discuss these implications, assumptions, and future directions.

The probability of hemiplasy due to introgression

A multitude of studies have revealed the potential role of introgression in shaping phenotypic convergence and adaptation (e.g. Heliconius Genome Consortium 2012, Huerta-Sanchez et al. 2014, Jones et al. 2018, Mullen et al. 2020). However, such studies rarely consider how introgression could lead to false inferences of convergence, due to hemiplasy at both the

molecular and phenotypic levels, if left unaccounted for. Our model results show that both ILS and introgression must be accounted for in order to make robust inferences of convergent evolution.

Our model for the probability of hemiplasy with introgression, combining concepts from two previously published models, also shares most of their assumptions. First, we have assumed the simplest possible introgression scenario, involving a single pair of species and with introgression occurring instantaneously at some point in the past. However, much more complex introgression scenarios are possible, including: introgression between multiple species pairs, involving ancestral populations (and internal branches), at multiple time points in the past, or continuously over a period of time. It is not always clear how the probability of hemiplasy would be affected under these alternative introgression scenarios. For example, we assume that the taxa sharing the derived state are also the ones involved in introgression, but introgression between other species pairs could alter patterns of discordance and therefore affect the hemiplasy risk. Many of these scenarios could be incorporated into the general MSNC framework as additional parent trees, but with more complex histories this may become mathematically intractable even in the three-taxon case (though our hemiplasy inference tool, *HeIST*, can help in this regard). Despite this limitation, we can generally expect that introgression will increase the overall risk of hemiplasy whenever rates of introgression are higher between pairs of species that also share the derived state for an incongruent trait. This is because what truly matters is the generation of gene tree topologies with internal branches where hemiplastic transitions can occur; the increased variance in coalescence times under more complex introgression scenarios, while affecting mutation probabilities, should have a comparatively minor effect (Figure 4).

We also assume that the coalescence times and gene tree frequencies of loci underlying trait variation follow neutral expectations. However, alleles controlling trait variation are often under some form of selection. Directional selection on such variation will reduce N_e relative to neutral expectations, which will decrease the rate of incomplete lineage sorting and consequently hemiplasy due to ILS. Of course, the rate of ILS used in our simulations is not taken directly from neutral expectations, but rather is estimated from real data. Therefore, the effects of selection on traits of interest will only be manifest if they are greater than the general effects of linked selection across the regions used to estimate discordance (cf. Kern and Hahn 2018). On the other hand, introgressed alleles can lead to hemiplasy even in cases where there is no ILS. In fact, directional selection would also make it more likely that introgressed loci have a discordant topology, as it reduces ILS within parent trees 2 and 3. Alternatively, balancing selection can maintain ancestral polymorphism and increase rates of discordance due to ILS. This will also increase the risk of hemiplasy (e.g. Fontaine et al. 2015, Lamichhaney et al. 2016, Palesch et al. 2018).

Considerations for the inference tool *HeIST*

While the software we introduce here allows for multiple novel types of inferences, it also has several limitations that are important to address. First, errors common to all phylogenetic methods can be introduced into the user-specified species tree at several steps, including errors in the tree topology, concordance factors, and branch lengths (via both the conversion to coalescent

units and tree smoothing). If concordance factors are underestimates—for instance, due to errors in gene tree reconstruction—then the branch lengths in coalescent units will also be underestimates of their true values. The result would be simulations with more ILS and discordance than actually occurred. In cases where there are concerns about branch length estimates, we suggest running *HeIST* with a range of values. Second, the process of smoothing the coalescent tree introduces additional error in branch length estimates. Specific internal branches that are very short may have their length increased; conversely, long internal branches may be shortened. The lengthening of internal branches relevant to understanding the hemiplasy risk may decrease the overall rate of discordance, and make inferences about hemiplasy from *HeIST* conservative. Third, when researchers have questions about hemiplasy involving either very large phylogenies or very low mutation rates, only a small number of simulated trees may match the incongruent pattern found in real data. The large number of simulations required may not be computationally feasible, though careful pruning of species that do not affect inferences of hemiplasy may greatly reduce this limitation. Finally, while *HeIST* can simulate phylogenies with introgression, it requires that the timing, direction, and rate of each introgression event is provided. To obtain this information, we recommend using a phylogenetic network-based approach such as PhyloNet (Wen et al. 2018), SNaQ (Solís-Lemus and Ané 2016), or SpeciesNetwork (Zhang et al. 2018).

One issue that concerns both our theoretical work and *HeIST* is the specification of the mutation rate. In both, cases, we assume that the rates of $0 \rightarrow 1$ and $1 \rightarrow 0$ transitions are equivalent, and that these rates are constant across the tree under study. Violations of these assumptions will certainly influence the probabilities of hemiplasy and homoplasy, though it is unlikely that underlying mutation rates will vary substantially among closely related lineages (Lynch 2010). More importantly, these rates represent the mutation rate among character states, and may not always be the same as nucleotide mutation rates. We have assumed in the results presented here that transitions between character states are controlled by a single site, and therefore that the nucleotide mutation rate is a good approximation of the trait mutation rate. However, the degree to which this is true will depend on the genetic architecture underlying a trait. For example, transitions in floral color are often underlain by loss of function mutations, and many mutational targets can potentially lead to the same phenotypic changes (Rausher 2008, Smith & Rausher 2011). In such cases, the rate of trait transitions can potentially be many times higher than the nucleotide mutation rate, with homoplasy becoming more probable as a result. In contrast, trait transitions can also require multiple molecular changes, the order of which may be constrained by pleiotropy and epistasis. Such changes underlie, for instance, high-altitude adaptation of hemoglobin in mammals (Storz et al. 2009, Tufts et al. 2015). In these cases, the rate of trait transitions may be many times lower than the nucleotide mutation rate, with hemiplasy becoming more probable as a result.

Evolution of green-blooded lizards

In our analysis of lizards in the genus *Prasinohaema*, we found strong support for one or two independent origins of green blood from a red-blooded ancestor, with two origins being the most likely. This contrasts with analyses that do not account for gene tree discordance, in which four

transitions is the best explanation. These results strongly suggest that hemiplasy has played a role in the evolution of green blood.

Applying *HeIST* to this clade involves some system-specific assumptions. First, it invokes the potentially strong assumption that the green-blooded phenotype is achievable by a single mutation. While the physiological mechanism for this phenotype is well-understood (Austin & Jessing, 1994), the genetic architecture underlying the transition from a red-blooded ancestor is not. As discussed in the previous section, this architecture will affect the choice of θ used as the trait evolutionary rate in our simulations. Since the genetic architecture is unknown, our choice of θ was based on what is typically observed for nucleotide mutations in vertebrate systems (Lynch 2006).

Another key assumption is that the gene trees and concordance factors estimated from the UCE dataset are accurate, as is the regression approach for converting branch length units. The observed R^2 of 0.554 for the unit conversion in this dataset might be interpreted as surprisingly low given that it is a regression of the same quantity measured in two different units. This value likely reflects uncertainty generated in several steps of our analysis, including the estimation of branch lengths in the maximum-likelihood species tree, and the procedure of randomly sampling quartets to estimate sCFs used by IQ-TREE. Nonetheless, it is high enough to ensure that tip branches estimated in coalescent units are proportionally similar to those in the maximum-likelihood tree, suggesting that the regression approach works well as an approximation. In addition, the regression line appears to slightly over-estimate very short branch lengths in coalescent units, making our inferences of hemiplasy conservative.

Conclusions

A major question in the study of convergent evolution is whether phenotypic convergence is underlain by convergent changes at the molecular level (Storz 2016). The work presented here is concerned primarily with such molecular changes, and the results of our analysis of green-blooded lizards demonstrate that apparently convergent phenotypes can arise from a single molecular change. Such shared changes come about as a result of gene tree discordance due to ILS, introgression, or some combination of the two. Given that these phenomena are common in phylogenomic datasets (Pollard et al. 2006, Fontaine et al. 2015, Pease et al. 2016, Novikova et al 2016, Wu et al. 2018), perhaps it should be less surprising that phylogenetically incongruent traits often have a common genetic basis.

Finally, while the tools presented here may help to rule out cases of molecular convergence, the observation of a single molecular origin for a trait does not rule out the occurrence of convergent adaptation in general. Parallel selective pressures from the environment on the same molecular variation may be regarded as one of many possible modes of convergent evolution (Lee & Coop 2017). In studying novel phenotypes like the evolution of green blood, there is still tremendous interest in understanding the ecological pressures that may have led to the independent fixation of single, ancestral changes along multiple lineages. In general, integrative approaches combining modern phylogenomics with an ecological context will pave the way toward an improved understanding of the nature of convergent evolution.

Acknowledgements

We thank Rafael Guerrero, Leonie Moyle, and Ben Fulton for helpful comments and advice. We also thank Zachary Rodriguez for sharing the lizard data. This work was supported by National Science Foundation grant DEB-1936187.

FIGURES

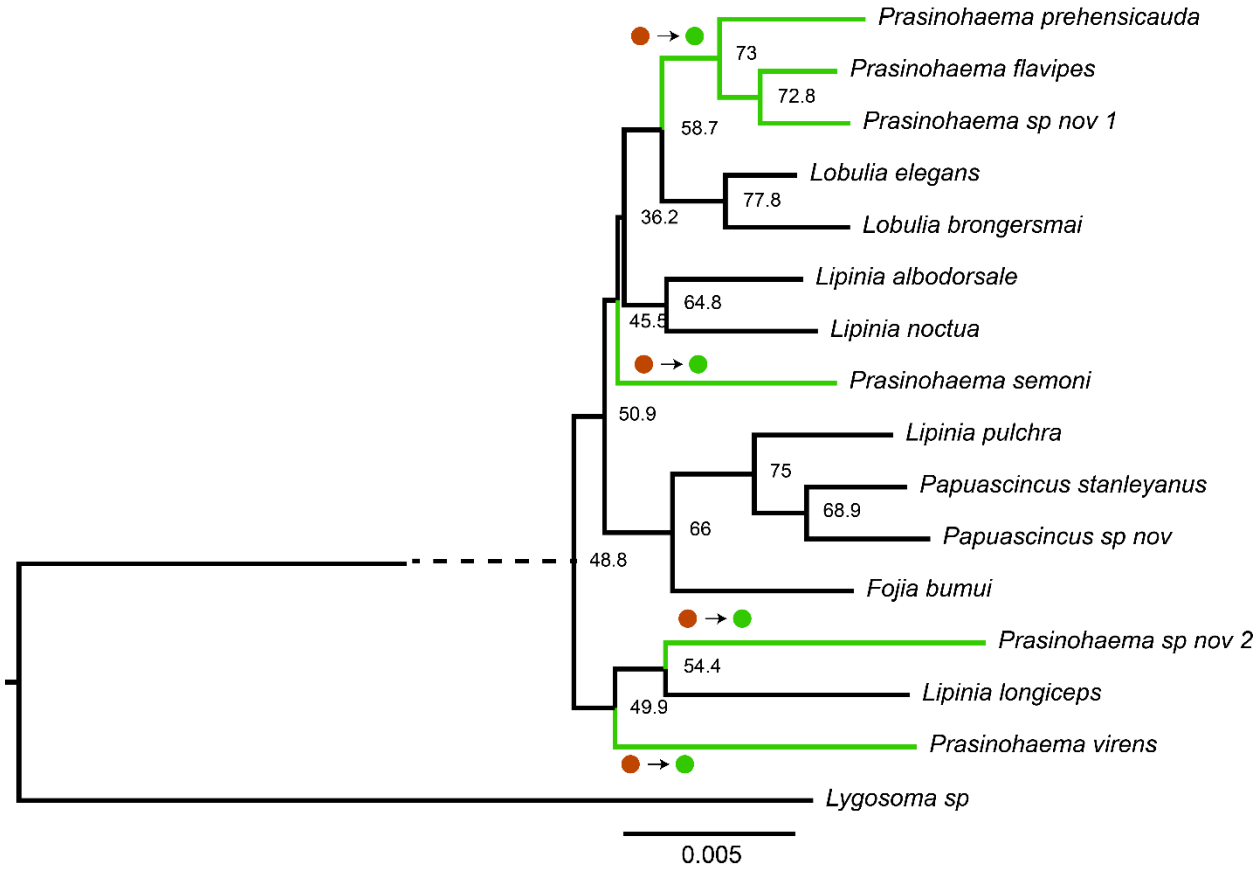

Figure 1: Maximum-likelihood species tree of the clade including green-blooded lizards and an outgroup, constructed from the concatenation of 3220 ultra-conserved elements (data from Rodriguez et al. 2018). Branch lengths are shown in units of substitutions per site. Taxa with green blood are labelled in green. The most parsimonious transitions to green blood from a red-blooded ancestor, given the species tree, are also labelled. The length of the branch to the root (dashed line) is not shown to scale for clarity. Nodes are labelled with site concordance factors.

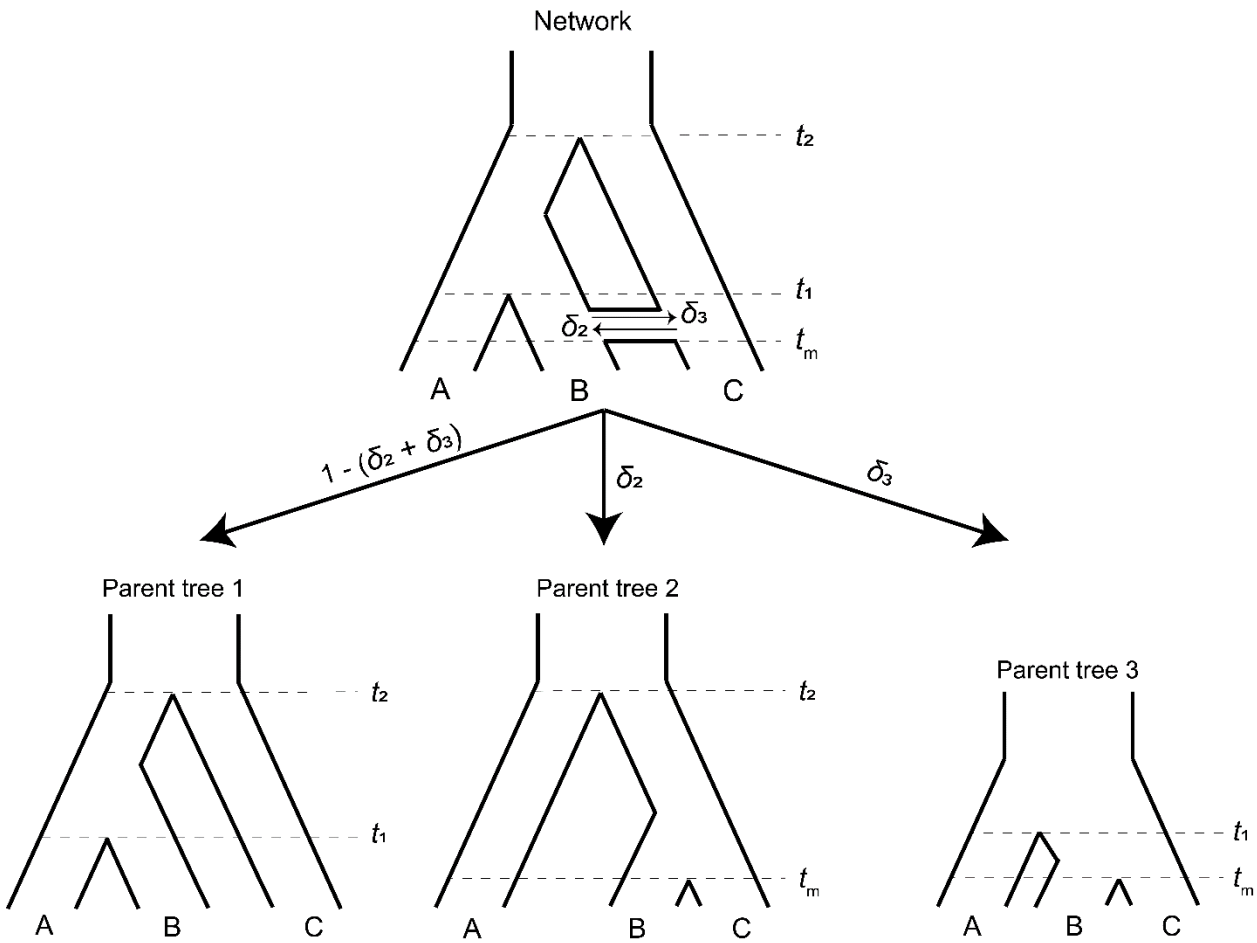

Figure 2: A phylogenetic network (top) can be split into a set of parent trees (bottom) representing the possible histories at individual loci. The probability that a locus is described by a particular parent tree depends on the genomic rate of introgression (arrow labels).

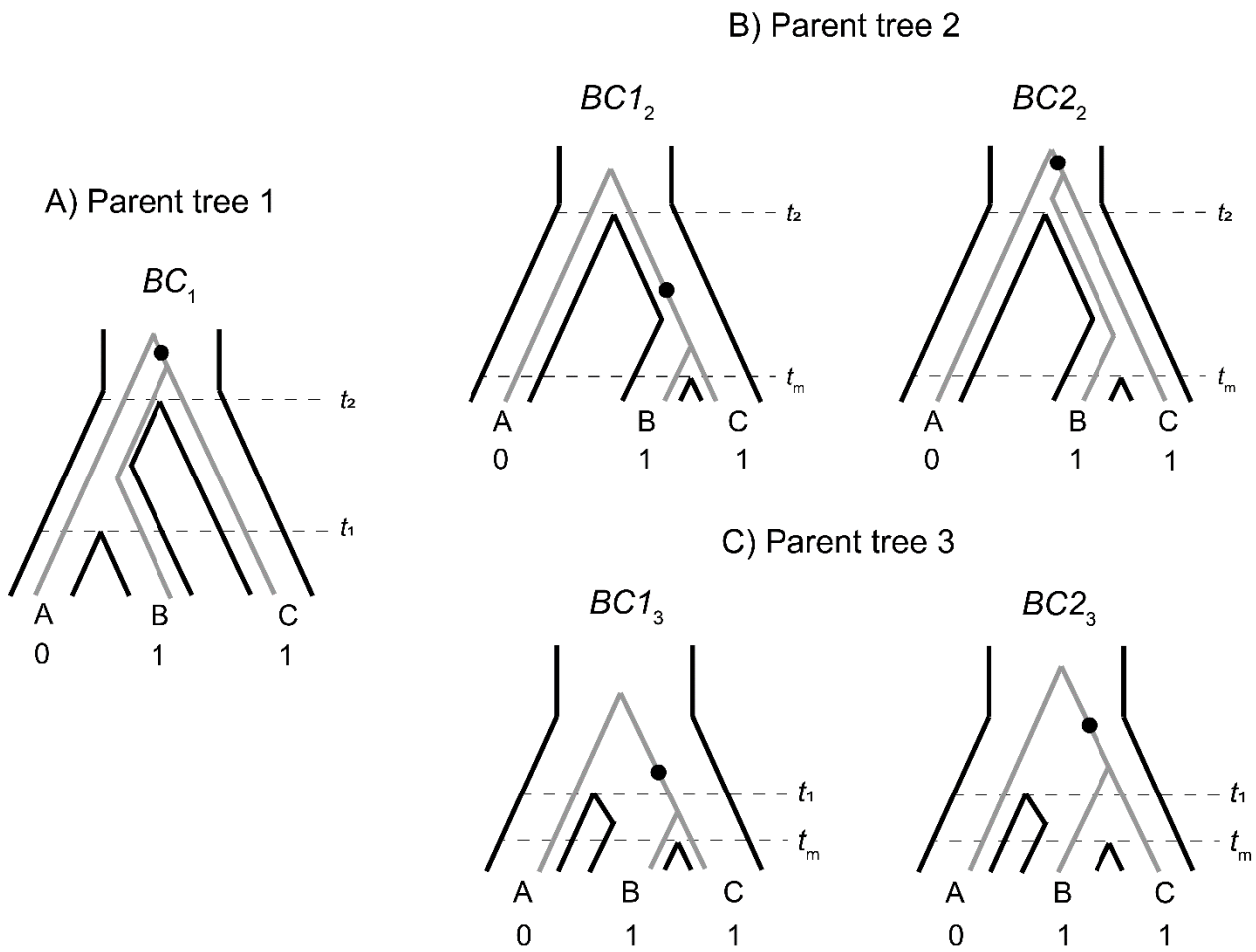

Figure 3: The possible paths to hemiplasy under the multispecies network coalescent. All cases require a transition on the internal branch of a gene tree with the topology ((B,C),A). In parent tree 1 (panel A), only one such possible gene tree exists (shown in grey; BC_1). In both parent trees 2 and 3 (panels B and C respectively), there are two possible gene trees with this topology. These gene trees differ in internal branch lengths, depending on the parent tree of origin and whether the tree is the result of lineage sorting ($BC1_2$ and $BC1_3$) or incomplete lineage sorting ($BC2_2$ and $BC2_3$) within introgressed histories.

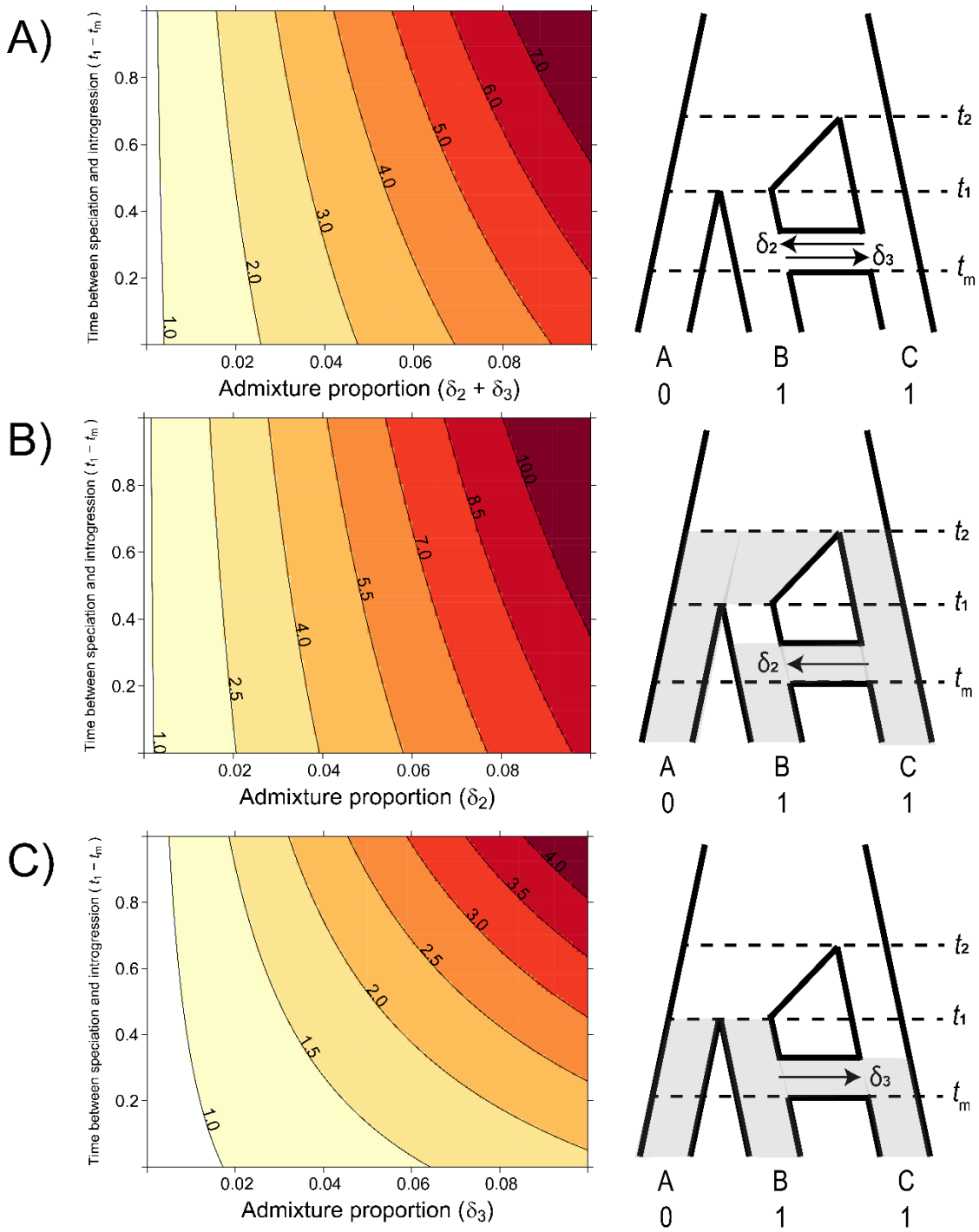

Figure 4: The probability of hemiplasy relative to homoplasy (contours) as a function of the admixture proportion (x-axis), the time between speciation and introgression (y-axis), and the direction of introgression (panels). At x = 0 in each panel, P_e / P_o = 0.818. A) Equal rates of introgression in both directions. B) Introgression in only the C → B direction. C) Introgression in only the B → C direction.

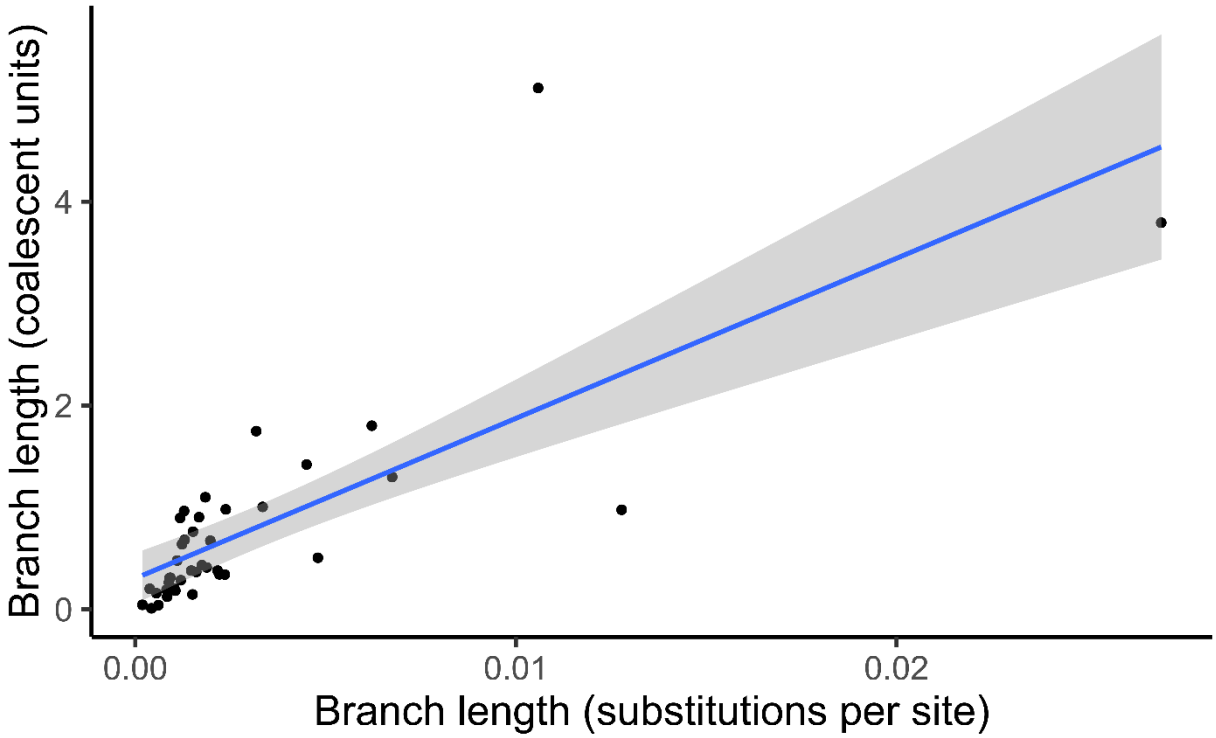

Figure 5: Regression of internal branch lengths in units of substitutions per site (x-axis) on the length of the same branch in coalescent units (2*N* generations, as estimated from site concordance factors) (y-axis), for the full New Guinea lizard phylogeny.

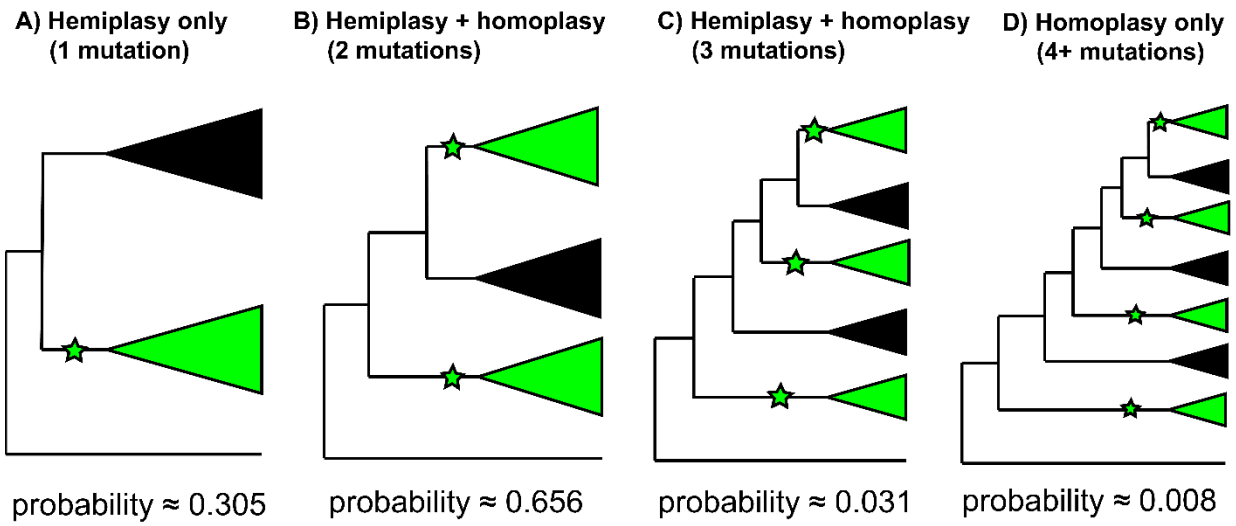

Figure 6: Probable histories for the origin of green blood in New Guinea lizards calculated using *HeIST*. Trees depict the maximum number of clades expected for gene tree topologies under each scenario, with green-blooded clades in green, and branches with transitions to green blood labelled with stars. Exactly which species are sorted into these clades can vary, meaning many possible gene trees exist for each of the four depicted scenarios. Reported probabilities are based on 10^{10} simulated trees with mutations, with probabilities conditional on matching the empirical distribution of green-blooded species within the simulated datasets.

REFERENCES

Ané, C., Larget, B., Baum, D. A., Smith, S. D., & Rokas, A. (2007). Bayesian estimation of concordance among gene trees. Molecular Biology and Evolution, 24(2), 412-426. doi:10.1093/molbev/msl170

Avise, J. C., & Robinson, T. J. (2008). Hemiplasy: A new term in the lexicon of phylogenetics. Systematic Biology, 57(3), 503-507. doi:10.1080/10635150802164587

Brandvain, Y., Kenney, A. M., Flagel, L., Coop, G., & Sweigart, A. L. (2014). Speciation and introgression between *Mimulus nasutus* and *Mimulus guttatus*. PLoS Genetics, 10(6), e1004410. doi:10.1371/journal.pgen.1004410

Copetti, D., Burquez, A., Bustamante, E., Charboneau, J. L. M., Childs, K. L., Eguiarte, L. E., . . . Sanderson, M. J. (2017). Extensive gene tree discordance and hemiplasy shaped the genomes of North American columnar cacti. Proceedings of the National Academy of Sciences of the United States of America, 114(45), 12003-12008. doi:10.1073/pnas.1706367114

Degnan, J. H. (2018). Modeling hybridization under the network multispecies coalescent. Systematic Biology, 67(5), 786-799. doi:10.1093/sysbio/syy040

Degnan, J. H., & Rosenberg, N. A. (2009). Gene tree discordance, phylogenetic inference and the multispecies coalescent. Trends in Ecology & Evolution, 24(6), 332-340. doi:10.1016/j.tree.2009.01.009

Delsuc, F., Brinkmann, H., & Philippe, H. (2005). Phylogenomics and the reconstruction of the tree of life. Nature Reviews Genetics, 6(5), 361-375. doi:10.1038/nrg1603

Dunn, C. W., Hejnol, A., Matus, D. Q., Pang, K., Browne, W. E., Smith, S. A., . . . Giribet, G. (2008). Broad phylogenomic sampling improves resolution of the animal tree of life. Nature, 452(7188), 745-749. doi:10.1038/nature06614

Durand, E. Y., Patterson, N., Reich, D., & Slatkin, M. (2011). Testing for ancient admixture between closely related populations. Molecular Biology and Evolution, 28(8), 2239-2252. doi:10.1093/molbev/msr048

Felsenstein, J. (1985). Phylogenies and the comparative method. The American Naturalist, 125(1), 1-15. doi:10.1086/284325

Felsenstein, J. (2004). Inferring Phylogenies. Sunderland, Massachusetts: Sinauer Associates.

Fitch, W. M. (1971). Toward defining the course of evolution: minimum change for a specific tree topology. Systematic Zoology, 20(4), 406-416. doi:10.2307/2412116

Fontaine, M. C., Pease, J. B., Steele, A., Waterhouse, R. M., Neafsey, D. E., Sharakhov, I. V., . . . Besansky, N. J. (2015). Extensive introgression in a malaria vector species complex revealed by phylogenomics. Science, 347(6217), 1258524. doi:10.1126/science.1258524

Gadagkar, S. R., Rosenberg, M. S., & Kumar, S. (2005). Inferring species phylogenies from multiple genes: concatenated sequence tree versus consensus gene tree. Journal of Experimental Zoology B: Molecular and Developmental Evolution, 304(1), 64-74. doi:10.1002/jez.b.21026

Green, R. E., Krause, J., Briggs, A. W., Maricic, T., Stenzel, U., Kircher, M., . . . Paabo, S. (2010). A draft sequence of the Neandertal genome. Science, 328(5979), 710-722. doi:10.1126/science.1188021

Guerrero, R. F., & Hahn, M. W. (2018). Quantifying the risk of hemiplasy in phylogenetic inference. Proceedings of the National Academy of Sciences of the United States of America, 115(50), 12787-12792. doi:10.1073/pnas.1811268115

Hahn, M. W., & Hibbins, M. S. (2019). A three-sample test for introgression. Molecular Biology and Evolution, 36(12), 2878-2882. doi:10.1093/molbev/msz178

Hahn, M. W., & Nakhleh, L. (2016). Irrational exuberance for resolved species trees. Evolution, 70(1), 7-17. doi:10.1111/evo.12832

Heliconius Genome Consortium. (2012). Butterfly genome reveals promiscuous exchange of mimicry adaptations among species. Nature, 487(7405), 94-98. doi:10.1038/nature11041

Hibbins, M. S., & Hahn, M. W. (2019). The timing and direction of introgression under the multispecies network coalescent. Genetics, 211(3), 1059-1073. doi:10.1534/genetics.118.301831

Hudson, R. R. (1983). Testing the constant-rate neutral allele model with protein sequence data. Evolution, 37(1), 203-217. doi:10.2307/2408186

Hudson, R. R. (2002). Generating samples under a Wright-Fisher neutral model of genetic variation. Bioinformatics, 18(2), 337-338. doi:10.1093/bioinformatics/18.2.337

Huerta-Sanchez, E., Jin, X., Asan, Bianba, Z., Peter, B. M., Vinckenbosch, N., . . . Nielsen, R. (2014). Altitude adaptation in Tibetans caused by introgression of Denisovan-like DNA. Nature, 512(7513), 194-197. doi:10.1038/nature13408

Joly, S., McLenachan, P. A., & Lockhart, P. J. (2009). A statistical approach for distinguishing hybridization and incomplete lineage sorting. The American Naturalist, 174(2), E54-70. doi:10.1086/600082

Jones, M. R., Mills, L. S., Alves, P. C., Callahan, C. M., Alves, J. M., Lafferty, D. J. R., . . . Good, J. M. (2018). Adaptive introgression underlies polymorphic seasonal camouflage in snowshoe hares. Science, 360(6395), 1355-1358. doi:10.1126/science.aar5273

Kern, A. D., & Hahn, M. W. (2018). The neutral theory in light of natural selection. Molecular Biology and Evolution, 35(6), 1366-1371. doi:10.1093/molbev/msy092

Lamichhaney, S., Han, F., Berglund, J., Wang, C., Almen, M. S., Webster, M. T., . . . Andersson, L. (2016). A beak size locus in Darwin's finches facilitated character displacement during a drought. Science, 352(6284), 470-474. doi:10.1126/science.aad8786

Lee, K. M., & Coop, G. (2017). Distinguishing among modes of convergent adaptation using population genomic data. Genetics, 207(4), 1591-1619. doi:10.1534/genetics.117.300417

Liu, K. J., Dai, J., Truong, K., Song, Y., Kohn, M. H., & Nakhleh, L. (2014). An HMM-based comparative genomic framework for detecting introgression in eukaryotes. PLoS Computational Biology, 10(6), e1003649. doi:10.1371/journal.pcbi.1003649

Lynch, M. (2006). The origins of eukaryotic gene structure. Molecular Biology and Evolution, 23(2), 450-468. doi:10.1093/molbev/msj050

Lynch, M. (2010). Evolution of the mutation rate. Trends in Genetics, 26(8), 345-352. doi:10.1016/j.tig.2010.05.003

Mallet, J., Besansky, N., & Hahn, M. W. (2016). How reticulated are species? Bioessays, 38(2), 140-149. doi:10.1002/bies.201500149

Mendes, F. K., & Hahn, M. W. (2016). Gene tree discordance causes apparent substitution rate variation. Systematic Biology, 65(4), 711-721. doi:10.1093/sysbio/syw018

Mendes, F. K., Hahn, Y., & Hahn, M. W. (2016). Gene tree discordance can generate patterns of diminishing convergence over time. Molecular Biology and Evolution, 33(12), 3299-3307. doi:10.1093/molbev/msw197

Meng, C., & Kubatko, L. S. (2009). Detecting hybrid speciation in the presence of incomplete lineage sorting using gene tree incongruence: a model. Theoretical Population Biology, 75(1), 35-45. doi:10.1016/j.tpb.2008.10.004

Minh, B. Q., Hahn, M. W., & Lanfear, R. (2018). New methods to calculate concordance factors for phylogenomic datasets. BioRxiv. doi:https://doi.org/10.1101/487801

Minh, B. Q., Schmidt, H. A., Chernomor, O., Schrempf, D., Woodhams, M. D., von Haeseler, A., & Lanfear, R. (2020). IQ-TREE 2: New models and efficient methods for phylogenetic inference in the genomic era. Molecular Biology and Evolution (in press). doi:10.1093/molbev/msaa015

Misof, B., Liu, S. L., Meusemann, K., Peters, R. S., Donath, A., Mayer, C., . . . Zhou, X. (2014). Phylogenomics resolves the timing and pattern of insect evolution. Science, 346(6210), 763-767. doi:10.1126/science.1257570

Mullen, S. P., VanKuren, N. W., Zhang, W., Nallu, S., Kristiansen, E. B., Wuyun, Q., . . . Kronforst, M. R. (2020). Disentangling population history and character evolution among hybridizing lineages. Molecular Biology and Evolution (in press). doi:10.1093/molbev/msaa004

Nguyen, L. T., Schmidt, H. A., von Haeseler, A., & Minh, B. Q. (2015). IQ-TREE: a fast and effective stochastic algorithm for estimating maximum-likelihood phylogenies. Molecular Biology and Evolution, 32(1), 268-274. doi:10.1093/molbev/msu300

Novikova, P. Y., Hohmann, N., Nizhynska, V., Tsuchimatsu, T., Ali, J., Muir, G., . . . Nordborg, M. (2016). Sequencing of the genus *Arabidopsis* identifies a complex history of nonbifurcating speciation and abundant trans-specific polymorphism. Nature Genetics, 48(9), 1077-1082. doi:10.1038/ng.3617

Palesch, D., Bosinger, S. E., Tharp, G. K., Vanderford, T. H., Paiardini, M., Chahroudi, A., . . . Silvestri, G. (2018). Sooty mangabey genome sequence provides insight into AIDS resistance in a natural SIV host. Nature, 553(7686), 77-81. doi:10.1038/nature25140

Pamilo, P., & Nei, M. (1988). Relationships between gene trees and species trees. Molecular Biology and Evolution, 5(5), 568-583. doi:10.1093/oxfordjournals.molbev.a040517

Patterson, N., Moorjani, P., Luo, Y. T., Mallick, S., Rohland, N., Zhan, Y. P., . . . Reich, D. (2012). Ancient admixture in human history. Genetics, 192(3), 1065-1093. doi:10.1534/genetics.112.145037

Pease, J. B., Haak, D. C., Hahn, M. W., & Moyle, L. C. (2016). Phylogenomics reveals three sources of adaptive variation during a rapid radiation. PLoS Biology, 14(2), e1002379. doi:10.1371/journal.pbio.1002379

Pease, J. B., & Hahn, M. W. (2015). Detection and polarization of introgression in a five-taxon phylogeny. Systematic Biology, 64(4), 651-662. doi:10.1093/sysbio/syv023

Pollard, D. A., Iyer, V. N., Moses, A. M., & Eisen, M. B. (2006). Widespread discordance of gene trees with species tree in Drosophila: Evidence for incomplete lineage sorting. PLoS Genetics, 2(10), 1634-1647. doi:10.1371/journal.pgen.0020173

Rambaut, A., & Grassly, N. C. (1997). Seq-Gen: An application for the Monte Carlo simulation of DNA sequence evolution along phylogenetic trees. Computer Applications in the Biosciences, 13(3), 235-238. doi:10.1093/bioinformatics/13.3.235

Rausher, M. D. (2008). Evolutionary transitions in floral color. International Journal of Plant Sciences, 169(1), 7-21. doi:10.1086/523358

Reich, D., Thangaraj, K., Patterson, N., Price, A. L., & Singh, L. (2009). Reconstructing Indian population history. Nature, 461(7263), 489-494. doi:10.1038/nature08365

Rodriguez, Z. B., Perkins, S. L., & Austin, C. C. (2018). Multiple origins of green blood in New Guinea lizards. Science Advances, 4(5), eaao5017. doi:10.1126/sciadv.aao5017

Smith, S. D., & Rausher, M. D. (2011). Gene loss and parallel evolution contribute to species difference in flower color. Molecular Biology and Evolution, 28(10), 2799-2810. doi:10.1093/molbev/msr109

Stamatakis, A. (2014). RAxML version 8: a tool for phylogenetic analysis and post-analysis of large phylogenies. Bioinformatics, 30(9), 1312-1313. doi:10.1093/bioinformatics/btu033

Storz, J. F. (2016). Causes of molecular convergence and parallelism in protein evolution. Nature Reviews Genetics, 17(4), 239-250. doi:10.1038/nrg.2016.11

Storz, J. F., Runck, A. M., Sabatino, S. J., Kelly, J. K., Ferrand, N., Moriyama, H., . . . Fago, A. (2009). Evolutionary and functional insights into the mechanism underlying high-altitude adaptation of deer mouse hemoglobin. Proceedings of the National Academy of Sciences of the United States of America, 106(34), 14450-14455. doi:10.1073/pnas.0905224106

Tufts, D. M., Natarajan, C., Revsbech, I. G., Projecto-Garcia, J., Hoffmann, F. G., Weber, R. E., . . . Storz, J. F. (2015). Epistasis constrains mutational pathways of hemoglobin adaptation in high-altitude pikas. Molecular Biology and Evolution, 32(2), 287-298. doi:10.1093/molbev/msu311

Wen, D., Yu, Y., & Nakhleh, L. (2016). Bayesian inference of reticulate phylogenies under the multispecies network coalescent. PLoS Genetics, 12(5), e1006006. doi:10.1371/journal.pgen.1006006

Wen, D., Yu, Y., Zhu, J., & Nakhleh, L. (2018). Inferring phylogenetic networks using PhyloNet. Systematic Biology, 67(4), 735-740. doi:10.1093/sysbio/syy015

Wu, M., Kostyun, J. L., Hahn, M. W., & Moyle, L. C. (2018). Dissecting the basis of novel trait evolution in a radiation with widespread phylogenetic discordance. Molecular Ecology, 27(16), 3301-3316. doi:10.1111/mec.14780

Yu, Y., Degnan, J. H., & Nakhleh, L. (2012). The probability of a gene tree topology within a phylogenetic network with applications to hybridization detection. PLoS Genetics, 8(4), e1002660. doi:10.1371/journal.pgen.1002660

Yu, Y., Dong, J., Liu, K. J., & Nakhleh, L. (2014). Maximum likelihood inference of reticulate evolutionary histories. Proceedings of the National Academy of Sciences of the United States of America, 111(46), 16448-16453. doi:10.1073/pnas.1407950111

Zhang, C., Rabiee, M., Sayyari, E., & Mirarab, S. (2018). ASTRAL-III: polynomial time species tree reconstruction from partially resolved gene trees. BMC Bioinformatics, 19(6), 153. doi:10.1186/s12859-018-2129-y